Pharm Res (2011) 28:166–176
DOI 10.1007/s11095-010-0271-y

RESEARCH PAPER

Suprachoroidal Drug Delivery to the Back of the Eye Using Hollow Microneedles

Samirkumar R. Patel • Angela S. P. Lin • Henry F. Edelhauser • Mark R. Prausnitz

Received: 26 February 2010 / Accepted: 2 September 2010 / Published online: 21 September 2010

ABSTRACT

Purpose In this work, we tested the hypothesis that microneedles provide a minimally invasive method to inject particles into the suprachoroidal space for drug delivery to the back of the eye.

Methods A single, hollow microneedle was inserted into the sclera, and infused nanoparticle and microparticle suspensions into the suprachoroidal space. Experiments were performed on whole rabbit, pig, and human eyes *ex vivo*. Particle delivery was imaged using brightfield and fluorescence microscopy as well as microcomputed tomography.

Results Microneedles were shown to deliver sulforhodamine B as well as nanoparticle and microparticle suspensions into the suprachoroidal space of rabbit, pig, and human eyes. Volumes up to 35 μL were administered consistently. Optimization of the delivery device parameters showed that microneedle length, pressure, and particle size played an important role in determining successful delivery into the suprachoroidal space. Needle lengths of 800–1,000 μm and applied pressures of 250–300 kPa provided most reliable delivery.

Conclusions Microneedles were shown for the first time to deliver nanoparticle and microparticle suspensions into the suprachoroidal space of rabbit, pig and human eyes. This shows that microneedles may provide a minimally invasive method for controlled drug delivery to the back of the eye.

KEY WORDS eye suprachoroidal space · hollow microneedle · microparticle · nanoparticle · ocular drug delivery

INTRODUCTION

The leading causes of blindness in the industrialized world are diseases that affect the back of the eye (1). These diseases include age-related macular degeneration (AMD), diabetic retinopathy, and uveitis, among others. Many pharmacological therapies exist to combat these diseases, but there are limited options for delivering these drugs effectively to their targets in the posterior segment of the eye. Delivering drugs to the posterior segment is challenging primarily because of difficult access to the target tissues and the eye's natural barriers that prevent foreign material from moving into them. The target tissues vary depending on the disease and sometimes even the stage of the disease, but are often the choroid and retina, as in the case of AMD, diabetic retinopathy, and uveitis (2,3). Therefore, an effective drug delivery system targeting the back of the eye would provide a significant improvement in the management of these vision-threatening diseases.

An effective drug delivery system for the back of the eye should embody four general characteristics. First, it should be minimally invasive and safe, so as to avoid complications caused by the procedure. Second, the drug should be administered in such a way that it is well targeted to the desired tissues and limits exposure to other regions of the

S. R. Patel · M. R. Prausnitz (✉)
School of Chemical and Biomolecular Engineering
Georgia Institute of Technology
311 Ferst Drive, Atlanta, Georgia 30332-0100, USA
e-mail: prausnitz@gatech.edu

A. S. P. Lin
Woodruff School of Mechanical Engineering
Georgia Institute of Technology
Atlanta, Georgia 30332, USA

H. F. Edelhauser (✉)
Emory Eye Center
Emory University
Atlanta, Georgia 30322, USA

eye. This would allow for high bioavailability while reducing adverse events and toxicity in surrounding tissues. Third, it should be capable of sustained delivery of the drug to reduce the frequency of administration and allow for better therapeutic control. Finally, administration of the drug should be as simple as possible, requiring only a routine office visit or, ideally, permitting self administration. A simple, reliable procedure can help reduce errors and compliance problems. Current methods of drug delivery to the posterior segment cannot meet all of these requirements.

Current local posterior segment drug delivery methods can be characterized by two overarching strategies: periocular or intravitreal (4,5). The periocular strategy deposits a drug on the outer surface of the globe and either relies on diffusion, natural transport mechanisms of the eye, or an applied biophysical driving force (e.g. inotopohresis) to deliver the drug inward towards its intraocular target. Periocular methods are usually minimally invasive, but often suffer from poor targeting and limited sustained release capabilities. The intravitreal method involves placing the drug formulation directly into the vitreous of the eye; the drug can then diffuse outward towards the retina and choroid. This is often accomplished by an intravitreal injection or an implant, which introduces the drug directly into the back of the eye and can be designed for sustained release. However, intravitreal delivery is invasive, carries a risk of endophthalmitis, and often exposes unintended tissues to the drug.

In this study, we investigate the suprachoroidal space as a route to target delivery of drugs to the back of the eye. The suprachoroidal space is a potential space between the sclera and choroid that goes circumferentially around the eye (6,7). Previous studies employing surgical procedures to introduce catheters into this space have shown that drugs delivered into the suprachoroidal space can be targeted towards the choroid and retina because the suprachoroidal space is in direct contact with the choroid (8–11). Introduction of controlled release formulations into the suprachoroidal space could further enable long-term therapy. Access to the suprachoroidal space, however, is difficult, and the methods that have previously been studied are invasive and too complex to be performed as a simple office procedure (8–11). We hypothesize that hollow microneedles can provide a minimally invasive method to inject nanoparticles and microparticles into the suprachoroidal space for drug delivery to the back of the eye. Hollow microneedles are needles of micron dimensions that can infuse fluid into tissue with excellent spatial targeting. Fabrication and characterization of hollow microneedles have been extensively studied for drug delivery to the skin (12–16), including recent human studies administering insulin (17) and influenza vaccine (18). Another recent study showed that hollow microneedles can pierce hundreds of microns into the ocular tunic and inject small molecules and particles into the sclera and corneal stroma (19).

In this study, we seek to determine if microneedles can pierce to the base of the sclera and target the suprachoroidal space. Considering the four characteristics of an ideal posterior segment drug delivery system, suprachoroidal delivery using microneedles has the promise to be simple, minimally invasive, targeted, and able to achieve sustained release by injecting nanoparticles and microparticles encapsulating drug for slow release.

More specifically, this study determines whether hollow microneedles can deliver small molecules and particles to the suprachoroidal space of pig, rabbit, and human cadaver eyes. We further measure the effect of microneedle length, infusion pressure, and intraocular pressure on the delivery of particles ranging from 20 nm to 1,000 nm in diameter in pig eyes. Finally, we examine the role that particle size plays and the influence of ocular anatomical barriers on delivery to the suprachoroidal space. With this work, we show for the first time that microneedles are capable of delivering fluid and particles into the suprachoroidal space in a minimally invasive manner to deliver drugs to the back of the eye.

MATERIALS AND METHODS

Materials

Whole rabbit eyes (Pel-Freez Biologicals, Rogers, AR), pig eyes (Sioux-Preme Packing, Sioux Center, IA), and human eyes (Georgia Eye Bank, Atlanta, GA), all with the optic nerve attached, were shipped on ice and stored wet at 4°C for up to 3 days. Prior to use, eyes were allowed to come to room temperature, and any fat and conjunctiva were removed to expose the sclera.

Hollow microneedles were fabricated from borosilicate micropipette tubes (Sutter Instrument, Novato, CA), as described previously (19). A custom, pen-like device with a threaded cap was fabricated to position the microneedle and allow precise adjustment of its length. This device was attached to a micropipette holder (MMP-KIT, World Precision Instruments, Sarasota, FL) with tubing that was connected to a carbon dioxide gas cylinder for application of infusion pressure. The holder was attached to a micromanipulator (KITE, World Precision Instruments) which was used to control insertion of the microneedle into the sclera. Fig. 1a shows a hollow microneedle held in the device compared to the tip of a 30 gauge hypodermic needle.

Carboxylate-modified FluoSpheres (Invitrogen, Carlsbad, CA) were injected as 2 wt% solids suspension of

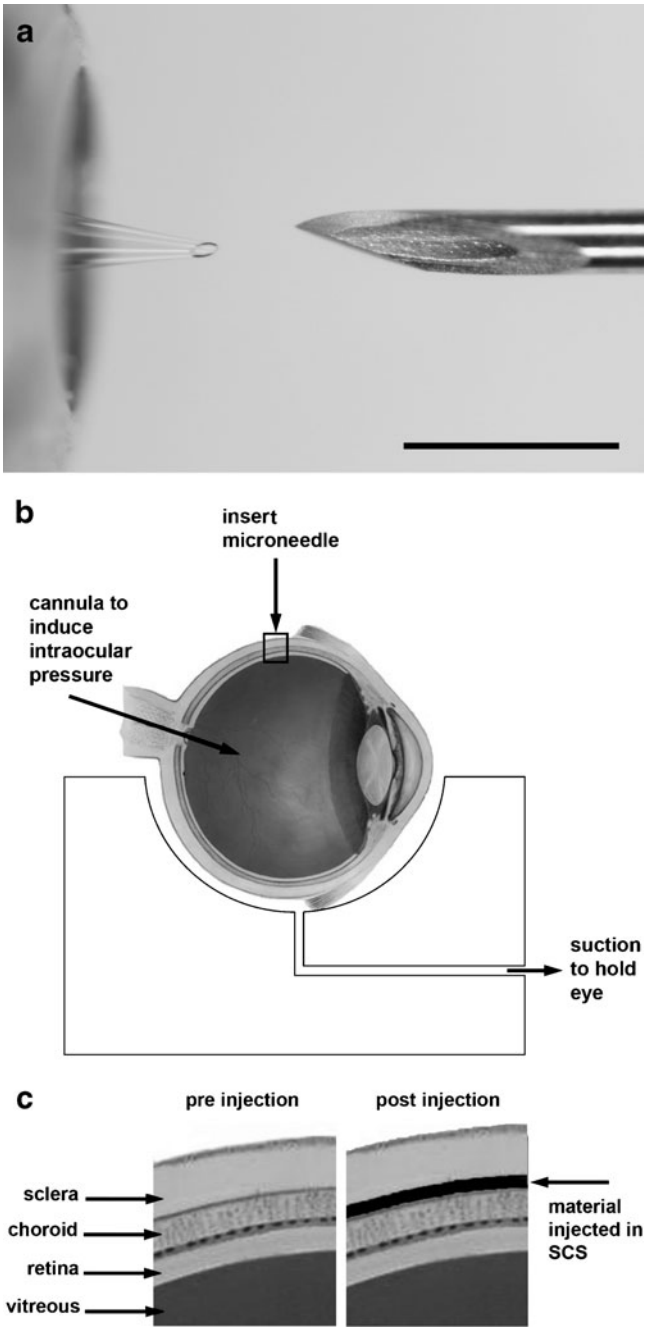

Fig. 1 Experimental approach to microneedle infusion into the suprachoroidal space. **a** Comparison of a hollow microneedle mounted in an insertion device (*above*) and the tip of a 30 gauge hypodermic needle (*below*). *Scale bar*: 1 mm. **b** Schematic diagram of the experimental set-up used to study suprachoroidal injection. The eye was placed on a custom-made mold with a channel through which suction was applied to hold the eye in place. A cannula inserted through the optic nerve of the eye allowed application of intraocular pressure. The microneedle was inserted into the sclera using the custom-made insertion device. **c** A magnified view of the boxed area in **b** shows an idealized schematic of the anatomy of the periocular tissues near the insertion site before and after the proposed suprachoroidal injection. Image of the eye was adapted from National Eye Institute, National Institutes of Health with permission.

20 nm, 100 nm, 500 nm, and 1,000 nm diameter particles. Tween 80 (Sigma-Aldrich, St. Louis, MO) at a final concentration of 0.5 wt% was added to the suspension and sonicated prior to use. Sulforhodamine B (Sigma-Aldrich) was dissolved in Hanks' balanced salt solution (Mediatech, Manassas, VA) to make a sulforhodmine solution of 10^{-4} M. Barium sulfate particles (Fisher Scientific, Waltham, MA) measuring 1 μm in diameter were suspended in balanced salt solution (BSS Plus, Alcon, Fort Worth, TX) to form a 1.5 wt% suspension.

Experimental Procedure

A custom acrylic mold, shaped to fit a whole eye, was built to hold the eye steady and used for all experiments (Fig. 1b). A catheter was inserted through the optic nerve into the vitreous and connected to a bottle of BSS Plus raised to a height to generate internal eye pressure of 18 mmHg unless otherwise specified. Suction was applied to a channel within the mold to hold the external surface of the eye steady during microneedle insertion and manipulation. Each microneedle was pre-filled using flexible quartz tubing (World Precision Instruments) with a desired volume of the material to be injected. The microneedle was placed in the device holder at a set microneedle length, attached to the micromanipulator and connected to the constant pressure source. Microneedles were then inserted perpendicular to the sclera tissue 5–7 mm posterior from the limbus. A set pressure was applied to induce infusion. Thirty seconds were allowed to see if infusion of the solution began. If infusion occurred, the pressure was stopped immediately upon injection of the specified volume. If visual observation of the injected material showed localization in the suprachoroidal space, the injection was considered a success. If infusion had not begun within that timeframe, then the applied pressure was stopped and the needle was retracted. This was considered an unsuccessful delivery.

Eyes to be imaged using microscopy were detached from the set-up within minutes after delivery was completed. The eyes were placed in acetone or isopentane which was kept on dry ice or liquid nitrogen, causing the eye to freeze completely within minutes after placement. The frozen eye was removed from the liquid, and portions of the eye were hand cut using a razor blade for imaging of injected material. Imaging was performed using a stereo microscope using brightfield and fluorescence optics (model SZX12, Olympus America, Center Valley, PA). The portions containing the sclera, choroid, and retina were placed in Optimal Cutting Temperature media (Sakura Finetek, Torrance, CA) and frozen under dry ice or liquid nitrogen. These samples were cryosectioned 10–30 μm thick (Microm Cryo-Star HM 560MV, Walldorf, Germany)

and imaged by brightfield and fluorescence microscopy (Nikon E600, Melville, NY) to determine the location of injected material in the eye. Images were collaged as necessary using Adobe Photoshop software (Adobe Systems, San Jose, CA).

Pig eyes used for microcomputed tomography imaging were not frozen after injection. Instead, pig eyes were injected with the barium sulfate suspension and stabilized in a 30 mm diameter sample tube and scanned in air using a Scanco μCT40 desktop conebeam system (Scanco Medical AG, Brüttisellen, Switzerland) at 30 μm isotropic voxel size, E = 55 kVp, I = 145 μA, and integration time = 200 ms. Through a convolution backprojection algorithm based on techniques from Feldkamp *et al.* (20), raw data were automatically reconstructed to generate 2D grayscale tomograms. Global segmentation values (Gauss sigma, Gauss support, and threshold) were chosen for the contrast-enhanced region as well as general eye tissue. Grayscale tomograms were stacked, and 3D binarized images were produced by applying the optimal segmentation values (one image for the entire eye and another for the region injected with contrast agent). These images were overlayed using Scanco image processing language to demonstrate the relative 3D position of the contrast-enhanced region within the entire eye.

RESULTS

Delivering to the Suprachoroidal Space Using a Hollow Microneedle

Because microneedles have not been used before to inject into the suprachoroidal space, we first wanted to determine if a liquid formulation could be delivered, what volume could be delivered, and over how large an area it would spread. We used red-fluorescent sulforhodamine B as a model compound and injected it into pig eyes *ex vivo* using a single hollow microneedle inserted just to the base of the sclera in order to target the suprachoroidal space. Using this approach, we found that it is possible to inject a liquid formulation into the suprachoroidal space and spread it circumferentially around the eye from a single microneedle injection, as discussed immediately below.

Fig. 2a shows a saggital cross-section of an untreated pig eye. The layers of the eye can be distinguished, and the white-colored sclera is in direct contact with the dark-colored layer that represents the choroid and retinal pigment epithelium. Fig. 2b shows a sagittal cross-section of a pig eye frozen after injection of 35 μL of sulforhodamine. The pink sulforhodamine solution can be seen selectively delivered just below the sclera and above the choroid. This region represents the suprachoroidal space and confirms that the solution was injected and spread within the suprachoroidal space from the initial injection site. We were able to inject volumes up to 35 μL without leakage, but larger volumes leaked out from openings on the surface of the eye where vortex veins would be attached *in vivo*. However, subsequent experiments in pigs and rabbits *in vivo* have demonstrated suprachoroidal delivery of up to 100 μL without leakage through these openings (data not shown).

We next wanted to determine if microneedles can also deliver particles into the suprachoroidal space, which is of interest for sustained-release drug delivery scenarios. We therefore injected particles with diameters of 500 nm or 1,000 nm into the suprachoroidal space of rabbit, pig, and human eyes *ex vivo* and imaged their distribution to confirm their localization just below the sclera. Cryosections of the rabbit eye were taken in the axial plane, and images were collaged to form a panoramic view, as shown in Fig. 3b. The images show the spread of the fluorescent (red/orange) particles along the equator of the eye in a thin sheath just below the sclera. In this experiment, a volume of 15 μL was injected, and in this particular cross-section taken in the plane of the insertion site, the injection has spread approximately 20 mm, which corresponds to about 36% of the total circumference of the eye.

As shown in Fig. 3c–d, cryosections of pig and human eyes were taken in the saggittal directions so that the images

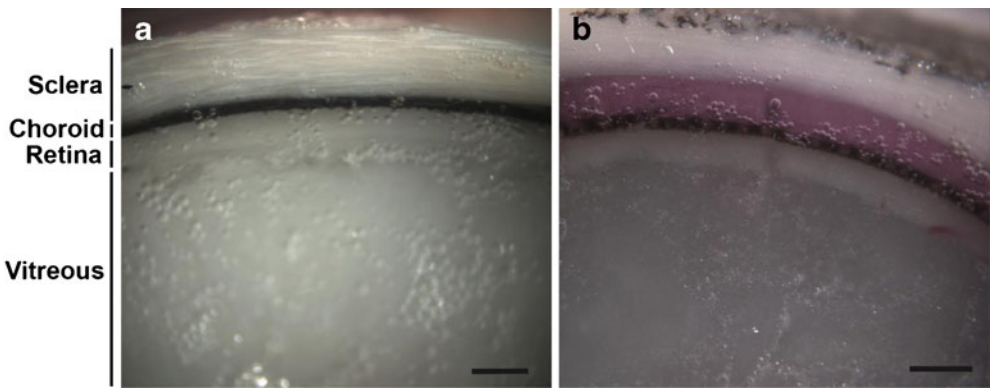

Fig. 2 Imaging of fluid infusion into the suprachoroidal space. Brightfield microscopic images of a cross-section of a frozen eye (**a**) showing normal ocular tissue including (1) sclera, (2) choroid, (3) retina and (4) vitreous humor and **b** showing the delivery of sulforhodamine B (*pink*) between the sclera and choroid (i.e., in the suprachoroidal space) *Scale bar*: 500 μm.

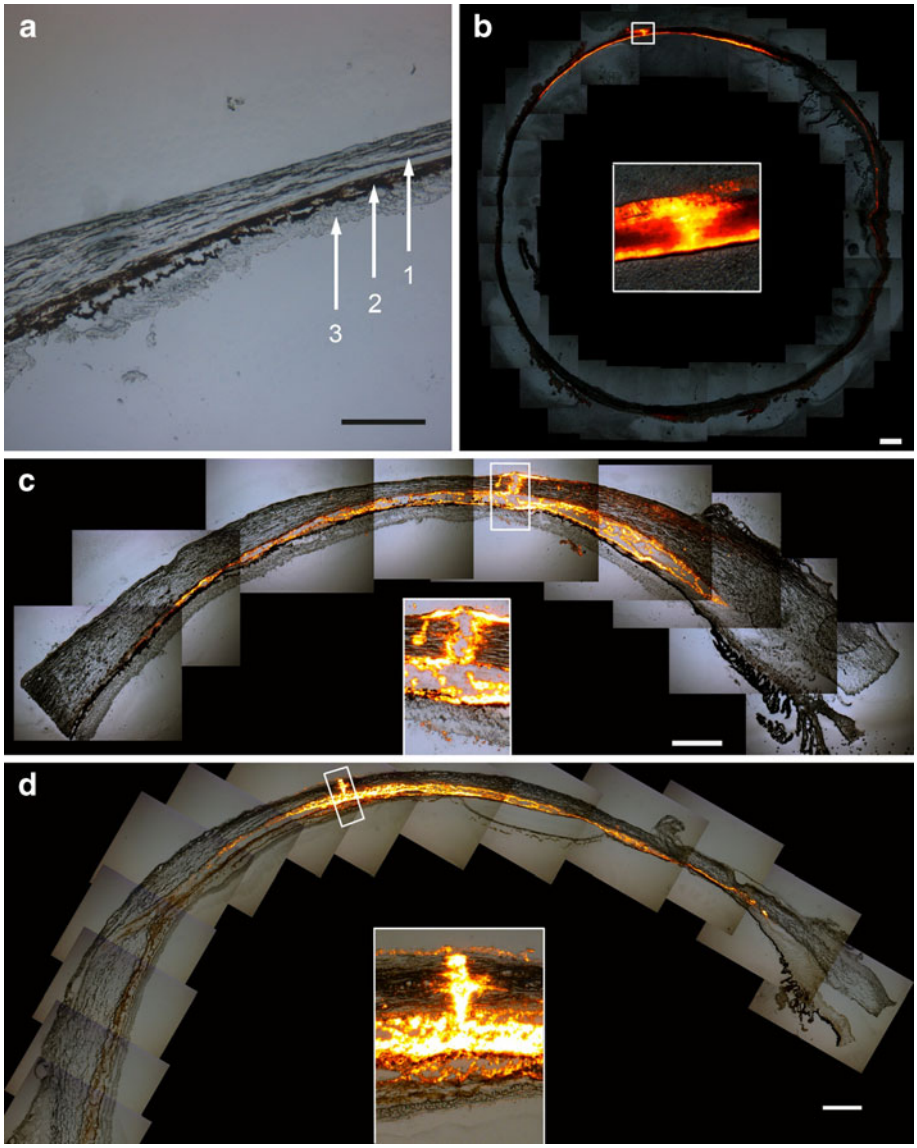

Fig. 3 Imaging of particle infusion into the suprachoroidal space. Image of a cryosection of a pig eye with no infusin into the suprachtroidal space (**a**). The layers of the eye are (1) sclera, (2) choroid, and (3) retina. Collaged fluorescence microscopy images of tissue cryosections show the delivery of **b** 500 nm particles into a rabbit eye, **c** 500 nm particles into a pig eye, and **d** 1,000 nm particles into a human eye, all *ex vivo*. Each image also displays an inset with a magnified view of the microneedle insertion site. These images show targeted delivery of particles into the suprachoroidal space and indicate that the microneedle did not penetrate into the choroid or retina. *Scale bar*: 500 μm.

show the anterior of the eye to the right and the posterior of the eye to the left. These images show the ability of microinjected particles to spread in the suprachoroidal space both in the anterior and posterior direction of the eye from the injection site. In these experiments, a single microneedle delivered 30 µL of a 2 wt% particle suspension into the suprachoroidal space of both species. Leakage was observed at the vortex vein openings away from the injection site similar to what was observed with sulforhodamine injections.

The insets in these images show magnified views of the microneedle insertion site. In each case, the insertion site within the sclera is filled with particles. In the case of the pig and human, the retina is still attached and visible, and it is clear that the microneedle has not penetrated to the retina. The rabbit retina separated during the cryosectioning procedure and is not visible. These results confirmed that a microneedle was able to target the suprachoroidal space of rabbit, pig, and human eyes to deliver particles up to 1,000 nm in diameter, which was the largest particle size used in this study. These particles spread from the injection site circumferentially in all directions within the suprachoroidal space.

To image the circumferential spread and localization of injected material in the suprachoroidal space in three dimensions using a noninvasive method, we utilized microcomputed tomography (µCT). After injecting 35 µL of 1 µm diameter barium sulfate contrast agent particles into the suprachoroidal space of a pig eye, cross-sectional images showed the particles distributed as a thin white strip that circled just below the outer edge of the eye, i.e., just below the sclera (Fig. 4a). This profile is characteristic of suprachoroidal delivery and similar to the results from fluorescence imaging. The three-dimensional reconstruction of

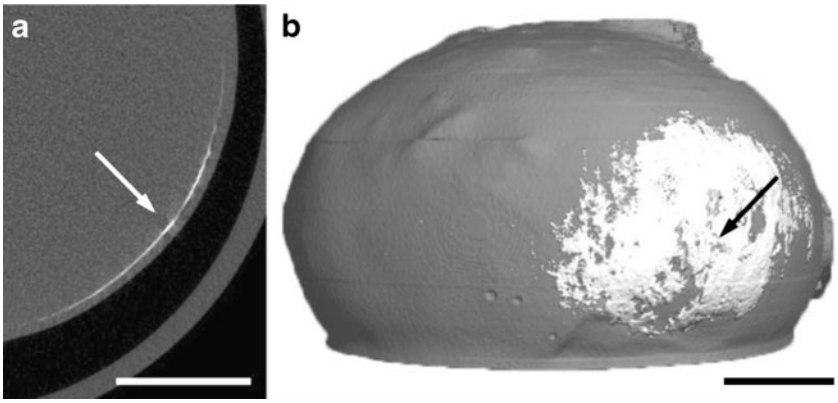

Fig. 4 Microcomputed tomography images of suprachoroidal delivery of barium sulfate particles. **a** Two-dimensional axial cross-section of a pig eye imaged after injection of 1 μm barium sulfate particles. The *arrow* points to the thin white strip of particles in the suprachoroidal space. **b** Two-dimensional cross-sections were reconstructed to form a three-dimensional map showing the distribution of particles, which have spread circumferentially in all directions around the microneedle insertion site (*arrow*) in the suprachoroidal space. *Scale bar*: 5 mm.

these cross-sectional images shows the spread of the particles in the posterior segment of the eye (Fig. 4b). The particle spread is approximately 5 mm in radius, although asymmetrically distributed around the injection site, and covers an approximate area of 70 mm^2, which represents 7% of the surface area of the back of the eye. This further confirms the ability of microneedles to spread particles over a significant portion of the posterior segment of the eye by targeting the suprachoroidal space.

Effect of Operating Parameters on Particle Delivery to the Suprachoroidal Space

We hypothesize that injection into the suprachoroidal space is facilitated by the use of longer microneedles, greater infusion pressure and smaller particle size. To test this hypothesis, we injected particles of 20, 100, 500, and 1,000 nm diameter into pig eyes *ex vivo* using a range of different microneedle lengths and infusion pressures to determine the success rate of suprachoroidal delivery. Our observation was that an attempted injection is either fully successful, as defined as complete injection of the 25 μL particle suspension into the suprachoroidal space, or as fully unsuccessful, as defined as an inability to inject at all. Partial injections were not observed. The success rates after five injection attempts at each condition are shown in Fig. 5.

In each of the graphs, the success rate increased with greater infusion pressure and with greater microneedle length (ANOVA, $p<0.05$). For the smallest particles (20 nm), 100% successful injections were achieved using a pressure of 250 kPa at all microneedle lengths. For 100 nm particles, the effects of pressure similarly plateued at 250 kPa, and 100% success was achieved at all but the shortest microneedle length (700 μm). For the larger particles (500 and 1,000 nm), the effects of pressure generally plateued at 300 kPa, and success rate significantly decreased for shorter microneedles.

We interpret these data in the following way. Short microneedle lengths inject within the sclera, such that particles must be forced through a portion of the sclera to reach the suprachoroidal space. Smaller particles (20 and 100 nm) can do this more easily, because the spacing of collagen fiber bundles in the sclera is on the order of 300 nm (21,22). The ground substance between the collagen fibers, which has a much smaller pore size (22), appear not to be rate limiting. However, larger particles (500 and 1,000 nm) have more difficulty crossing this anatomical barrier, such that infusion pressure becomes an important parameter and injection success rate decrease significantly.

Consistent with this hypothesis, statistical analysis in Table I shows that at a microneedle length of 700 μm, where the most scleral tissue must be traversed to reach the suprachoroidal space, success rate depended strongly on particle size. Using 800 and 900 μm microneedles, particles smaller than the collagen fiber spacing (20 and 100 nm) behaved similarly, and particles larger than the collagen fiber spacing (500 and 1,000 nm) also behaved similarly, but there was a significant difference between 100 nm and 500 nm particles. The longest microneedles (1,000 μm), which probably reach the base of the sclera, showed no significant dependence on particle size, suggesting that overcoming the collagen barrier in the sclera was no longer needed.

Our hypothesis further suggests that particles of 20 and 100 nm can spread within the sclera as well as the suprachoroidal space, whereas particles of 500 and 1,000 nm should localize exclusively in the suprachoroidal space. In Fig. 6, we compare the spread of 20 nm particles to 1,000 nm particles under identical conditions. As expected, the smaller particles exhibited significant spread in the sclera as well as the suprochoroidal space (Fig. 6a). In contrast, the larger particles are relegated primarily to the

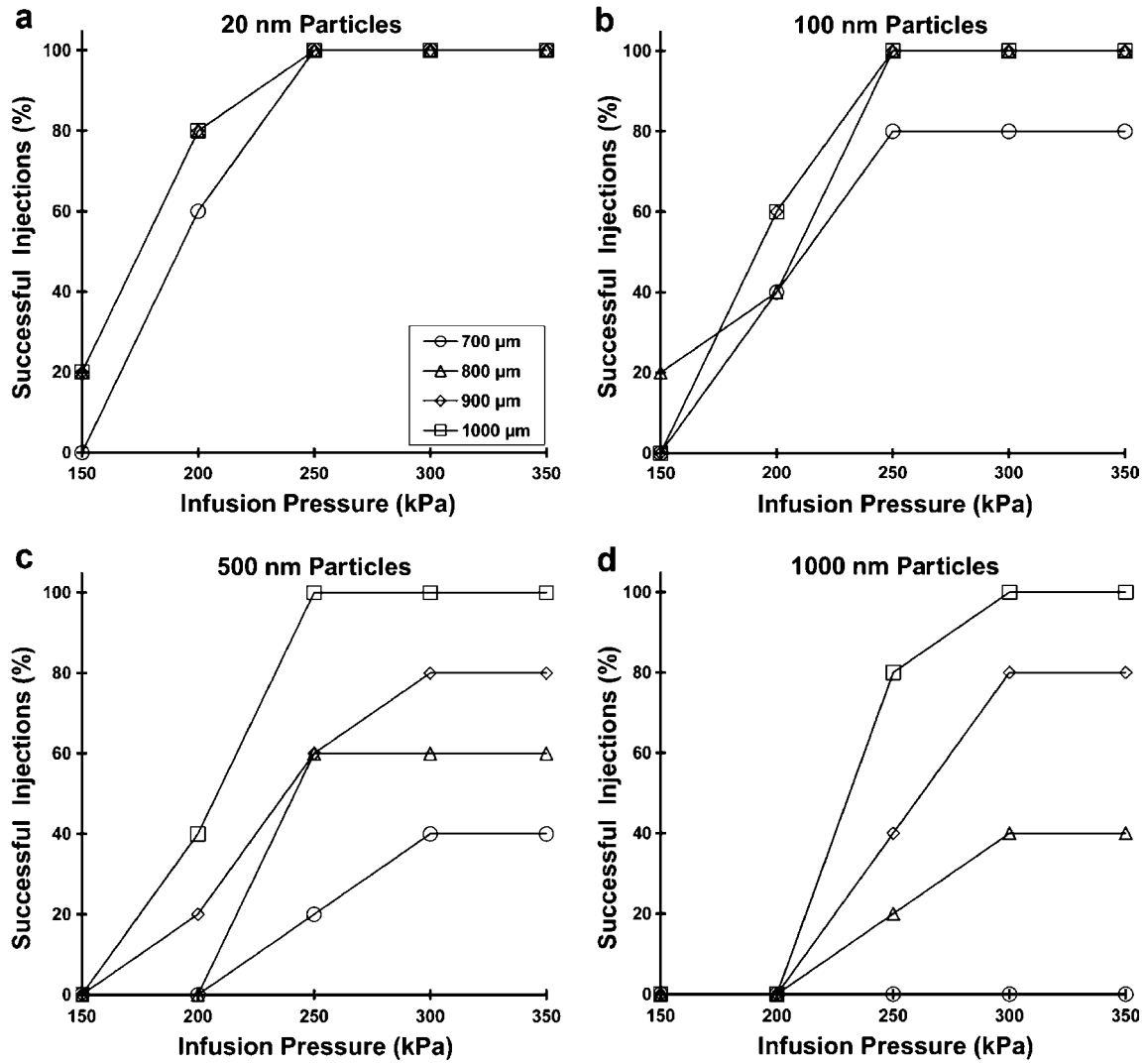

Fig. 5 The effect of infusion pressure and microneedle length on the success rate of suprachoroidal delivery for **a** 20 nm, **b** 100 nm, **c** 500 nm and **d** 1,000 nm particles into pig eyes. A total of five infusions were attempted at each condition studied. Increasing microneedle length and increasing infusion pressure increased the delivery success rate for all particle sizes (ANOVA $p < 0.05$).

suprachoroidal space and are largely excluded from the sclera (Fig. 6b). This localization of large particles is also consistent with results shown in Fig. 2, which includes additional data for 500 and 1,000 nm particles.

In summary, 20 and 100 nm particles were reliably injected using a minimum microneedle length of 800 µm and a minimum pressure of 250 kPa. To deliver 500 and 1,000 nm particles, a minimum microneedle length of 1,000 µm and a minimum pressure of 250–300 kPa were necessary.

Effect of Intraocular Pressure

We predict that an increase in intraocular pressure (IOP) should increase the success rate of particle delivery into the

Table I Statistical Comparison of Injection Success Rates of Particles of Different Sizes at Different Microneedle Lengths

Microneedle Length	20 *vs* 100 nm	100 *vs* 500 nm	500 *vs* 1,000 nm	20 *vs* 1,000 nm
700 µm	0.02*	0.02*	0.09	0.02*
800 µm	0.37	0.00*	0.10	0.01*
900 µm	0.18	0.03*	0.18	0.03*
1,000 µm	0.18	0.37	0.21	0.18

Values in table are p values determined using ANOVA. Significance was considered to be a $p < 0.05$ and indicated by an asterisk (*)

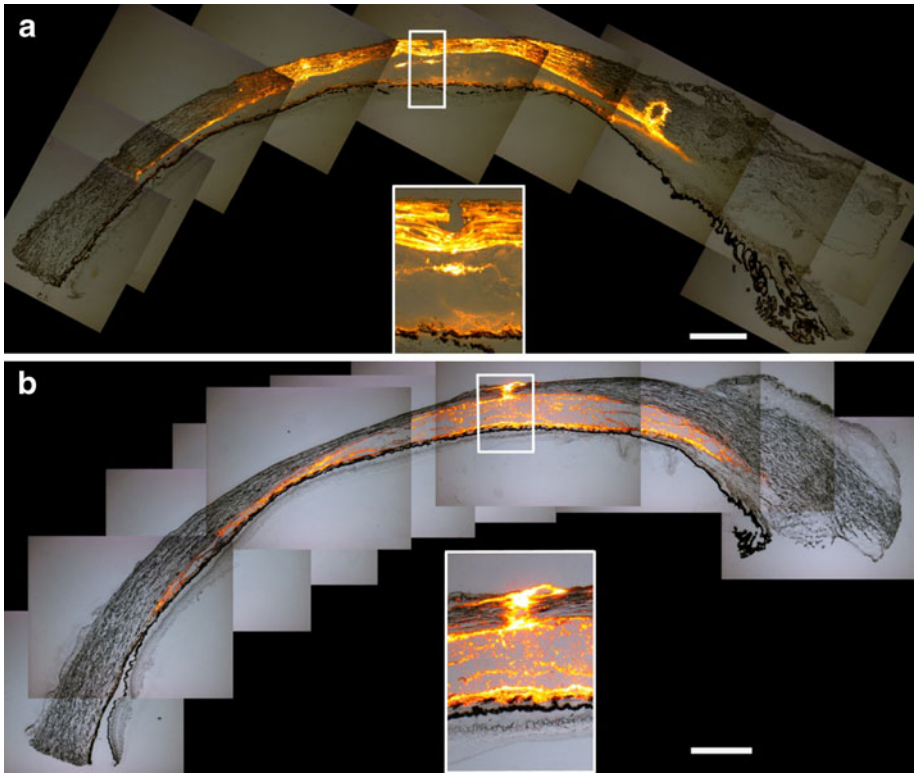

Fig. 6 Effect of particle size on particle distribution in the eye. Collaged fluorescence microscopy images of tissue cryosections show the delivery of **a** 20 nm particles and **b** 1,000 nm particles into the suprachoroidal space of pig eyes *ex vivo*. The images show that 20 nm particles spread in the suprachoroidal space and within the sclera. However, the 1,000 nm particles are primarily in the suprachoroidal space. The insertion sites are magnified in the insets. *Scale bar*: 500 μm.

suprachoroidal space. To clarify, IOP is the internal pressure within the eye that keeps the eye inflated. It provides a back pressure that can counteract the infusion pressure. However, our infusion pressures of 150–300 kPa are two orders of magnitude greater than the mean IOP in a normal adult of 15–16 mmHg (~2 kPa) (23), which means that IOP should contribute insignificant back pressure. Instead, we hypothesize that the main effect of elevated IOP is to make the sclera surface more firm, which reduces tissue surface deflection during microneedle insertion and thereby increases the depth of penetration into sclera for a microneedle of a given length. In a previous study, we similarly found that tissue deformation in the skin limited microneedle insertion depth (24).

To test this hypothesis, we injected 1,000 nm particles at two different levels of IOP, 18 and 36 mmHg. Consistent with our hypothesis, delivery success rate increased at elevated IOP, as shown in Fig. 7 (ANOVA, $p<0.05$). Notably, at normal IOP, no particles were delivered at the lowest infusion pressure (150 kPa) or using the shortest microneedles (700 μm), and only the longest microneedles (1,000 μm) achieved 100% success rate at the highest infusion pressure (300 kPa) (Fig. 7a). In contrast, at elevated IOP, particles were sometimes delivered at the lowest infusion pressure and using the shortest microneedles, and a 100% success rate was achieved using both 900 and 1,000 μm microneedles at the highest infusion pressure (Fig. 7b). Although we did not measure microneedle insertion depth directly, these results suggest that microneedle insertion may be more effective at elevated IOP because they insert deeper into the sclera and thereby increase infusion success rate.

DISCUSSION

This work introduced a minimally invasive strategy for drug delivery to the back of the eye. It showed that a hollow microneedle can inject liquid solution and suspensions of particles into the suprachoroidal space of rabbit, pig, and human eyes *ex vivo*. Suprachoroidal delivery represents an improvement over current periocular and intravitreal delivery methods, both of which are poorly targeted to the retinochoroidal sites of most posterior segment diseases. Rather than injecting drug outside the eye or in the vitreous humor, microneedle technology enables precisely targeted injection within the suprachoroidal space of the ocular tunic, which bathes the retinochoroidal surface with the drug formulation. Moreover, by taking advantage of the unique features of ocular anatomy, microneedle injection does not infuse the drug formulation in all directions from the injection site as in conventional injections. Instead, by targeting the suprachoroidal space, the drug formulation infuses circumferentially within the suprachoroidal space to cover a significant area of the back of the eye via a single injection.

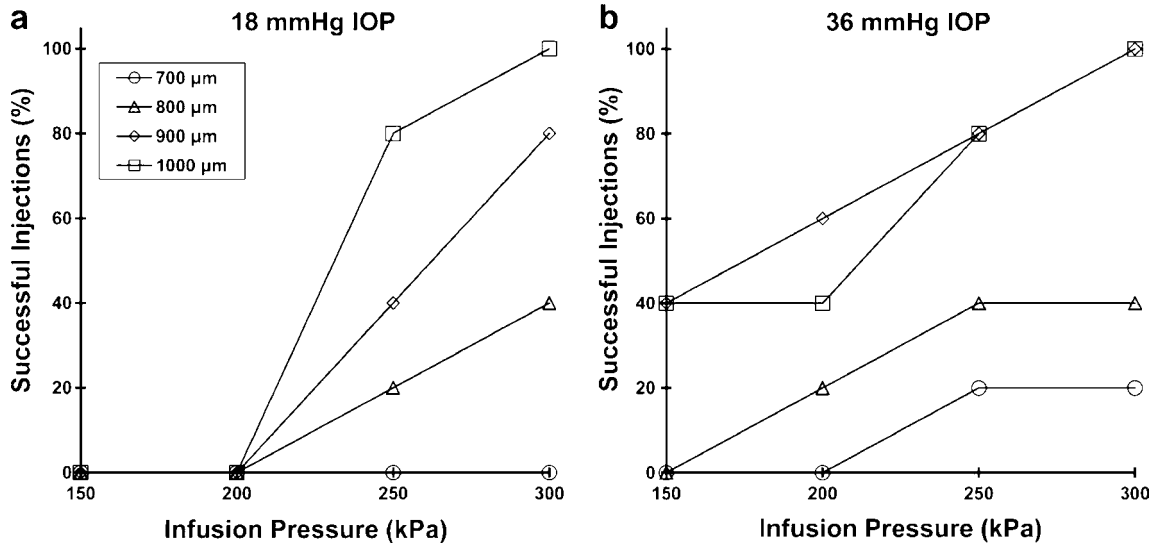

Fig. 7 The effect of infusion pressure and microneedle length on the success rate of suprachoroidal delivery of 1,000 nm particles at simulated IOP levels of **a** 18 mmHg and **b** 36 mmHg. A total of five infusions were attempted at each condition studied. The delivery success rate generally increased with an increase in IOP. IOP significantly affected delivery success rate as a function of infusion pressure when using 800, 900, and 1,000 μm long microneedles ($p < 0.05$).

This method of delivery has four important attributes of an effective drug delivery system for the posterior segment. First, the use of a hollow microneedle allows the delivery method to be minimally invasive, because the microneedle only penetrates hundreds of micrometers into the eye, which should protect the retina from mechanical damage and reduce the risk of infection. This is a significant improvement over past studies that have accessed the suprachoroidal space using much more invasive procedures (8–11) and may offer a safety profile similar to that of conventional intravitreal injection. Second, the suprachoroidal space offers the ability to target the choroid and retina by localizing the injection immediately adjacent to these tissues. Third, we showed the potential for sustained delivery by demonstrating injection of particles up to 1,000 nm in diameter into the suprachoroidal space. The ability of the suprachoroidal space to accommodate particles has not been previously reported. This finding suggests the possibility of injecting drug-loaded biodegradable particles into the suprachoroidal space for sustained drug release over a period of weeks to months, which could reduce the frequency of drug administration. Finally, the inherent safety and simplicity of microneedle injection suggest that suprachoroidal delivery could be carried out as a straightforward office procedure, rather than the surgical procedures required in previous suprachoroidal delivery studies (8–11).

This study further showed that microneedle length, particle size, and infusion pressure all affect the success rate of particle delivery to the suprachoroidal space. Notably, suprachoroidal injection was found to either occur fully or not to occur at all for any given injection attempt. This binary (i.e., all or nothing) response suggests that a critical event must occur to enable infusion, and we believe that critical event is the formation of a pathway from the microneedle tip to the suprachoroidal space through the sclera. Because microneedles appear to be inserted into, but not fully across, the sclera, particles must find a path through the remaining scleral tissue to reach the suprachoroidal space. This approach is advantageous because it minimizes mechanical damage to the eye and isolates the choroid and retina from the microneedle.

Our data indicates that smaller particles (20–100 nm) can more easily flow through scleral tissue because the sieving effect of the sclera's collagen fibers (19) allows smaller particles through but blocks larger particles (500–1,000 nm). The success rate is therefore increased by increasing microneedle length, which reduces the amount of scleral tissue between the microneedle and suprachoroidal space, and by increasing infusion pressure, which provides a greater driving force to push particles through the sclera. Increased microneedle length and infusion pressure were especially important for larger particles. Although an elevated IOP is not necessary for injection and neither is it desirable in patients, we found that elevated IOP also increased infusion success rate. We believe that elevated IOP reduced scleral surface deflection, which increased microneedle insertion depth and thereby reduced the amount of scleral tissue between the microneedle tip and the suprachoroidal space.

In this *ex vivo* study, we were able to inject volumes of 15–35 µL into the suprachoroidal space. Larger volumes led to leakage through vortex veins cut during excision of the eye from the animal, which we believe is an artifact of

the *ex vivo* model. These volumes are somewhat lower than typical intravitreal injections of 50–100 μL (25). However, previous studies on rabbits have shown that the suprachoroidal space can accommodate fluid up to several hundred microliters *in vivo* (26), which is supported by our preliminary data using microneedles in rabbits *in vivo* too (data not shown). We therefore conclude that volumes suitable to administer drug doses of use for ophthalmic applications can probably be administered using microneedle injection into the suprachoroidal space.

All experiments in this study were conducted on freshly excised animal and human cadaver eyes, which is an imperfect model for drug delivery *in vivo*. For example, the conjunctiva was not present on the eyes tested here, because the conjunctiva generally detaches once the eye is removed from the orbit. The presence of conjunctiva and tear fluid may affect microneedle insertion as additional layers the microneedle must penetrate to reach the suprachoroidal space. Additionally, the spread of solution and particles in the suprachoroidal space may be influenced by choroidal blood flow, which was not present during our experiments. For reference, Kim *et al.* showed that Gd-DTPA, with a molecular mass of ~1 kDa, is cleared from the suprachoroidal space within hours (10), which constrains the possibility of sustained drug delivery. However, particles are expected to be cleared much more slowly due to their much larger size than soluble molecules. Spread of a formulation within the suprachoroidal space will also be influenced by the viscosity of the formulation. Formulations that are more viscous than the water-like formulation used in these studies will most likely spread less within the suprachoroidal space. Detailed *in vivo* studies are needed to better understand the spread and clearance mechanisms from the suprachoroidal space.

In order for this delivery method to move toward clinical use, there are several issues that need to be addressed. For example, a microneedle insertion device and infusion system should be developed to enable the microneedle injection in a controlled manner. In addition, safety issues associated with injecting within the suprachoroidal space need to be addressed, especially if repeated injections are necessary. The current work shows a proof of concept for this ophthalmic drug delivery route, and additional work in these areas will help substantiate its potential as a feasible route for treating diseases of the back of the eye.

CONCLUSION

This work provides the first study to evaluate injection into the suprachoroidal space using a microneedle. It shows that this approach offers an attractive route to target the posterior segment of the eye in a simple, minimally invasive way. Delivery of particle formulations into the suprachoroidal space was facilitated by increasing infusion pressure, increasing microneedle length, increasing IOP, and decreasing particle size. Injecting particles in this way could enable sustained drug delivery from the suprachoroidal space and thereby reduce dosing frequency. Finally, this work determined the effect of operating parameters on particle infusion, coupled with mechanistic insight into the injection process, that can be used to design microneedle-based drug delivery systems for the suprachoroidal space.

ACKNOWLEDGEMENTS

We would like to thank Dr. Harvinder Gill and Dr. John Nickerson for helpful discussions and Donna Bondy for administrative support. This work was carried out at the Emory Eye Center and at the Center for Drug Design, Development and Delivery and the Institute for Bioengineering and Bioscience at Georgia Tech. This work was supported in part by the National Eye Institute (R24-EY-017045). M.R.P. serves as a consultant and is an inventor on patents licensed to companies developing microneedle-based products. This possible conflict of interest has been disclosed and is being managed by Georgia Tech and Emory University.

REFERENCES

1. del Amo EM, Urtti A. Current and future ophthalmic drug delivery systems: a shift to the posterior segment. Drug Discov Today. 2008;13:135–43.
2. Zarbin M, Szirth B. Current treatment of age-related macular degeneration. Optom Vis Sci. 2007;84:559–72.
3. Kimura H, Yasukawa T, Tabata Y, Ogura Y. Drug targeting to choroidal neovascularization. Adv Drug Deliv Rev. 2001;52:79–91.
4. Ghate D, Brooks W, McCarey BE, Edelhauser HF. Pharmacokinetics of intraocular drug delivery by periocular injections using ocular fluorophotometry. Invest Ophthalmol Vis Sci. 2007;48:2230–7.
5. Kim SH, Lutz RJ, Wang NS, Robinson MR. Transport barriers in transscleral drug delivery for retinal diseases. Ophthalmic Res. 2007;39:244–54.
6. Krohn J, Bertelsen T. Corrosion casts of the suprachoroidal space and uveoscleral drainage routes in the human eye. Acta Ophthalmol Scand. 1997;75:32–5.
7. Krohn J, Bertelsen T. Light microscopy of uveoscleral drainage routes after gelatine injections into the suprachoroidal space. Acta Ophthalmol Scand. 1998;76:521–7.
8. Einmahl S, Savoldelli M, D'Hermies F, Tabatabay C, Gurny R, Behar-Cohen F. Evaluation of a novel biomaterial in the suprachoroidal space of the rabbit eye. Invest Ophthalmol Vis Sci. 2002;43:1533–9.
9. Olsen TW, Feng X, Wabner K, Conston SR, Sierra DH, Folden DV, *et al.* Cannulation of the suprachoroidal space: a novel drug delivery methodology to the posterior segment. Am J Ophthalmol. 2006;142:777–87.

10. Kim SH, Galban CJ, Lutz RJ, Dedrick RL, Csaky KG, Lizak MJ, *et al.* Assessment of subconjunctival and intrascleral drug delivery to the posterior segment using dynamic contrast-enhanced magnetic resonance imaging. Invest Ophthalmol Vis Sci. 2007;48:808–14.
11. Gilger BC, Salmon JH, Wilkie DA, Cruysberg LP, Kim J, Hayat M, *et al.* A novel bioerodible deep scleral lamellar cyclosporine implant for uveitis. Invest Ophthalmol Vis Sci. 2006;47:2596–605.
12. Gardeniers H, Luttge R, Berenschot EJW, de Boer MJ, Yeshurun SY, Hefetz M, *et al.* Silicon micromachined hollow microneedles for transdermal liquid transport. J Microelectromech Syst. 2003;12:855–62.
13. Davis SP, Martanto W, Allen MG, Prausnitz MR. Hollow metal microneedles for insulin delivery to diabetic rats. IEEE Trans Biomed Eng. 2005;52:909–15.
14. Brazzle J, Papautsky I, Frazier AB. Micromachined needle arrays for drug delivery or fluid extraction. IEEE Eng Med Biol Mag. 1999;18:53–8.
15. Zahn JD, Talbot NH, Liepmann D, Pisano AP. Microfabricated polysilicon microneedles for minimally invasive biomedical devices. Biomed Microdev. 2000;2:295–303.
16. McAllister DV, Wang PM, Davis SP, Park JH, Canatella PJ, Allen MG, *et al.* Microfabricated needles for transdermal delivery of macromolecules and nanoparticles: fabrication methods and transport studies. Proc Natl Acad Sci USA. 2003;100:13755–60.
17. Gupta J, Felner EI, Prausnitz MR. Minimally invasive insulin delivery in subjects with type 1 diabetes using hollow microneedles. Diabetes Technol Ther. 2009;11:329–37.
18. Van Damme P, Oosterhuis-Kafeja F, Van der Wielen M, Almagor Y, Sharon O, Levin Y. Safety and efficacy of a novel microneedle device for dose sparing intradermal influenza vaccination in healthy adults. Vaccine. 2009;27:454–9.
19. Jiang J, Moore JS, Edelhauser HF, Prausnitz MR. Intrascleral drug delivery to the eye using hollow microneedles. Pharm Res. 2009;26:395–403.
20. Feldkamp LA, Davis LC, Kress JW. Practical cone-beam algorithm. J Opt Soc Am A Opt Image Sci Vis. 1984;1:612–9.
21. Meek KM, Fullwood NJ. Corneal and scleral collagens—a microscopist's perspective. Micron. 2001;32:261–72.
22. Edwards A, Prausnitz MR. Fiber matrix model of sclera and corneal stroma for drug delivery to the eye. AIChE J. 1998;44:214–25.
23. Klein BEK, Klein R, Linton KLP. Intraocular pressure in an American community—the beaver damn eye study. Invest Ophthalmol Vis Sci. 1992;33:2224–8.
24. Martanto W, Moore JS, Kashlan O, Kamath R, Wang PM, O'Neal JM, *et al.* Microinfusion using hollow microneedles. Pharm Res. 2006;23:104–13.
25. Peyman GA, Lad EM, Moshfeghi DM. Intravitreal injection of therapeutic agents. Retina. 2009;29:875–912.
26. Mittl RN, Tiwari R. Suprachoroidal injection of sodium hyaluronate as an 'internal' buckling procedure. Ophthalmol Res. 1987;19:255–60.